MNRAS **000**, 1–5 (2016) Preprint 22 July 2016 Compiled using MNRAS LATEX style file v3.0

High-energy gamma-ray observations of the accreting black hole V404 Cygni during its June 2015 outburst

A. Loh[1⋆], S. Corbel[1,2], G. Dubus[3,4], J. Rodriguez[1], I. Grenier[1], T. Hovatta[5,6], T. Pearson[7], A. Readhead[7], R. Fender[8] and K. Mooley[8]

[1] *Laboratoire AIM (CEA/IRFU - CNRS/INSU - Univ. Paris Diderot), CEA DSM/IRFU/SAp, F-91191 Gif-sur-Yvette, France*
[2] *Station de Radioastronomie de Nançay, Observatoire de Paris, PSL Research University, CNRS, Univ. Orléans, 18330 Nançay, France*
[3] *Univ. Grenoble Alpes, IPAG, F-38000 Grenoble, France*
[4] *CNRS, IPAG, F-38000 Grenoble, France*
[5] *Aalto University Metsähovi Radio Observatory, Metsähovintie 114, 02540 Kylmälä, Finland*
[6] *Aalto University Department of Radio Science and Engineering, P.O. BOX 13000, FI-00076 AALTO, Finland*
[7] *California Institute of Technology, 1200 E. California Blvd, MC 249-17, Pasadena, CA 91125, USA*
[8] *Astrophysics, Department of Physics, University of Oxford, Keble Road, Oxford OX1 3RH, UK*

arXiv:1607.06239v1 [astro-ph.HE] 21 Jul 2016

Accepted 2016 July 14. Received 2016 July 13; in original form 2016 April 22

ABSTRACT

We report on *Fermi*/Large Area Telescope observations of the accreting black hole low-mass X-ray binary V404 Cygni during its outburst in June–July 2015. Detailed analyses reveal a possible excess of γ-ray emission on 26 June 2015, with a very soft spectrum above 100 MeV, at a position consistent with the direction of V404 Cyg (within the 95% confidence region and a chance probability of 4×10^{-4}). This emission cannot be associated with any previously-known *Fermi* source. Its temporal coincidence with the brightest radio and hard X-ray flare in the lightcurve of V404 Cyg, at the end of the main active phase of its outburst, strengthens the association with V404 Cyg. If the γ-ray emission is associated with V404 Cyg, the simultaneous detection of 511 keV annihilation emission by INTEGRAL requires that the high-energy γ rays originate away from the corona, possibly in a Blandford-Znajek jet. The data give support to models involving a magnetically-arrested disk where a bright γ-ray jet can re-form after the occurrence of a major transient ejection seen in the radio.

Key words: black hole physics – stars: individual: V404 Cygni – gamma-rays: stars – radio continuum: stars – X-rays: binaries.

1 INTRODUCTION

The microquasars consist of an accreting black hole or neutron star in a binary system with transient or persistent relativistic jets (Mirabel & Rodríguez 1999). They display a wide range of behaviour at all wavelengths (e.g Fender 2006), but they have rarely been detected at high-energy γ rays, despite the high-energy particles produced in their jets (Corbel et al. 2002). Relativistic particles in the jet could emit γ rays, either by Compton up-scattering the low-energy photons from the accretion disc/stellar field (e.g. Georganopoulos et al. 2002; Bosch-Ramon et al. 2006) or by pion decays from inelastic collisions between jet particles and stellar wind protons (Romero et al. 2003). Gamma-ray photons could also be produced at the shock regions where the jets encounter the interstellar medium (Bosch-Ramon et al. 2011) or within the jet itself (Atoyan & Aharonian 1999). Despite their recurrent outbursts, only the microquasar Cyg X−3 (and perhaps Cyg X−1, Bodaghee et al. 2013; Malyshev et al. 2013) behaves like a clearly identified transient high-energy emitter (Fermi LAT Collaboration et al. 2009; Tavani et al. 2009). The latter's γ-ray flares are strongly correlated to the radio emission originating from the relativistic jets (Corbel et al. 2012). With a donor star of mass $>10\,M_\odot$, they are consistent with being high-mass X-ray binaries.

The low-mass X-ray binary (LMXB) V404 Cygni (also known as GS 2023+338) underwent an exceptional outburst phase in June 2015. V404 Cyg is a nearby system (2.39 ± 0.14 kpc, Miller-Jones et al. 2009) harbouring a $\sim 9\,M_\odot$ black hole and a $\sim 1\,M_\odot$ companion star (Khargharia et al. 2010; Wagner et al. 1992) with a 6.5-day orbital period (Casares et al. 1992). After a 26 year long quiescent period (e.g. Rana et al. 2016), renewed activity was detected with the *Swift*/BAT (Barthelmy et al. 2015) and *Fermi*/GBM (Younes 2015; Jenke et al. 2016, up to 300 keV) on June, 15 (MJD 57188). This triggered a worldwide multi-wavelength

⋆ E-mail: alan.loh@cea.fr

© 2016 The Authors

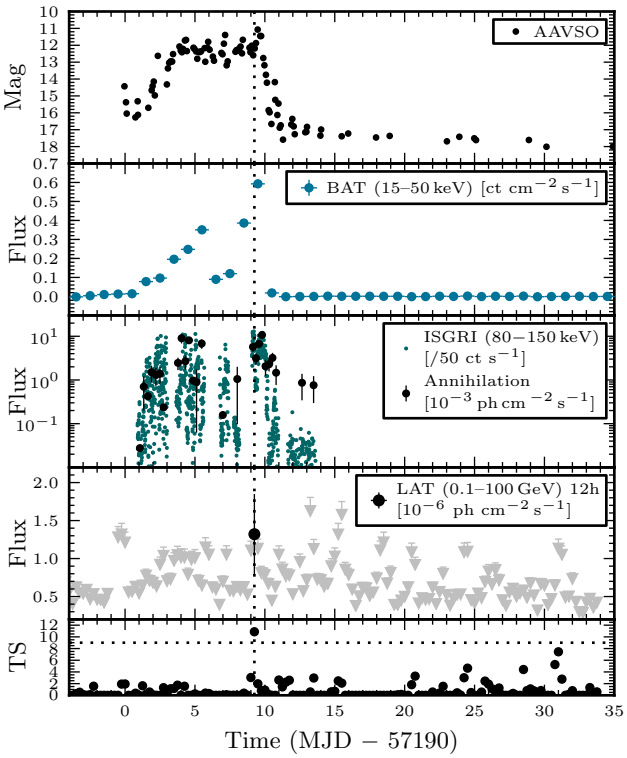

Figure 1. γ-ray flux and 95% upper limits >100 MeV and corresponding TS at the position of V404 Cyg in 12-h bins, shifted by 6 hours in time. The upper panels display the optical (extracted from the AAVSO database), hard X-ray *Swift*/BAT (Krimm et al. 2013), INTEGRAL/ISGRI count rate in the 80–150 keV band and the photon flux in the annihilation line (Siegert et al. 2016) LCs.

monitoring campaign from radio (Mooley et al. 2015) to hard X-rays (Rodriguez et al. 2015a) until V404 Cyg faded towards its quiescent accretion level in August 2015 (Sivakoff et al. 2015). The source has since undergone a fainter re-brightening, in December 2015 (e.g. Beardmore et al. 2015).

We took advantage of the intense activity and monitoring of V404 Cyg to probe its high-energy emission with the Large Area Telescope (LAT, Atwood et al. 2009) on board *Fermi*. The γ-ray analysis leading to the marginal detection of a flare is described in §2. Its origin is discussed in §3.

2 OBSERVATIONS AND DATA ANALYSIS

We have analysed the Pass 8 *Fermi*/LAT data covering the period 4 August 2008 to 17 July 2015. We used the *Fermi* Science Tools (version v10r1p1) with the Instrument Response Functions set `P8R2_SOURCE_V6`. A 15° acceptance cone centered on the infrared position of V404 Cyg has been considered. LAT photons labelled as `SOURCE` (`evclass=128`) were selected in the energy range from 100 MeV to 100 GeV. Events were also filtered based on the quality of the PSF, choosing the 3 best partitions (PSF 1 to 3: `evtype=56`) and standard filters on the data quality were applied. To minimise the contamination by Earth limb photons, γ-ray events with reconstructed directions pointing above a 90° zenith angle have been excluded.

In order to first constrain the emission of the whole region (nearby point-like sources and diffuse sky components), we performed a `binned` maximum-likelihood spectral analysis using the `NewMinuit` optimization algorithm implemented in `gtlike`. In the modelling of the region of interest (RoI), we have included the standard templates for the Galactic and isotropic backgrounds (`gll_iem_v06.fits` and `iso_P8R2_SOURCE_V6_v06.txt`[1]) and we used the spectral models listed in the 4-year *Fermi* catalogue (Acero et al. 2015, hereafter 3FGL) for all the sources within a 25° radius. The normalisation parameters were left free to vary for the diffuse components and for the sources either within 5° from the RoI center or labelled as variable (i.e. a variability index greater than 72.44, 3FGL). The results of the `binned` likelihood analysis using 7 years of LAT data, without including V404 Cyg which is not detected over this time scale, are fully consistent with those of the 3FGL catalogue. For instance, the flux normalisation for the blazar B2023+336 (3FGL J2025.2+3340, Kara et al. 2012), which is only ∼0.°32 away from V404 Cyg, differs by only ∼3% from the catalogue value. In addition, the residual maps do not show any noticeable structures, especially around the Galactic plane.

2.1 Gamma-ray variability

To study the shortest time-scale variations, we have fixed every source model parameter at their fitted values from the `binned` analysis and added a point-source at the location of V404 Cyg, modelled as a power-law with free normalisation and index. `Unbinned` analyses over 12 or 6-h bins were performed, with each bin shifted by 6 or 1-h from the previous one respectively (see Fig. 1 and 2). Whenever the derived Test Statistic (TS[2]) value was lower than 9 (corresponding to $\lesssim 3\sigma$ detection significance, Mattox et al. 1996), we computed 95 per cent upper limits on the high-energy flux using the method of Helene (1991) as implemented in the `pyLikelihood` module of the Science Tools. Otherwise, integrated γ-ray fluxes along with 1σ statistical error bars are provided. The LAT exposure (averaged on 12 h) ranges between 1 and 4×10^7 cm^2 s during the considered period, anti-correlated with the flux upper limits in Fig. 1, and is $\sim 2.5 \times 10^7$ cm^2 s during the γ-ray excess on MJD 57199.2.

Our variability analysis (performed between MJD 57140 and 57225) encompassing the June outburst period of V404 Cyg reveals the presence of a weak γ-ray excess at a location close to the LMXB around MJD 57199 (26 June 2015). The date of the γ-ray excess maximum statistical significance is estimated at MJD 57199.2 ± 0.1 (based on our 6-hour bins, see Fig. 2), although we caution that the measurements are not independent since the bins overlap in exposure. At the position of V404 Cyg, we measure a peak photon flux $F_\gamma = (2.3 \pm 0.8) \times 10^{-6}$ ph cm^{-2} s^{-1}, using the 6-hour bins (quoted errors are statistical and dominate the systematic uncertainties), for a corresponding TS value of 15.3 (the maximum on 12-hour bins is $F_\gamma = (1.4 \pm 0.5) \times 10^{-6}$ ph cm^{-2} s^{-1} for TS = 15.2, see Fig. 3). The spectrum is very soft and scales as $F_\gamma \propto E^{-3.5 \pm 0.8}$.

[1] http://fermi.gsfc.nasa.gov/ssc/data/analysis/
[2] TS = $2 \ln(\mathcal{L}_1/\mathcal{L}_0)$, $\mathcal{L}_1$ and $\mathcal{L}_0$ are the likelihood maxima with or without including the target source into the model.

As a verification procedure, we have computed the 12-h bin lightcurve (LC) of the closest *Fermi* source: 3FGL J2025.2+3340, with the normalisation of its spectral component let free to vary and excluding V404 Cyg from the model. This blazar underwent one flaring episode in July 2009 which lasted tens of days (*Fermi* All-sky Variability Analysis, Ackermann et al. 2013) and is labelled as variable in the 3FGL catalogue (with a variability index of 278.7, Kara et al. 2012; Ackermann et al. 2015). Its LC shows no significant detection over the 30 days encompassing the outburst period of the LMXB. The highest value (TS∼8.1) occurs on MJD 57199.25, which is consistent with the observed γ-ray excess since some of the photons are attributed to the blazar's emission if V404 Cyg is not taken into account. Furthermore, we note that no multi-wavelength activity has been reported from this source despite intense monitoring of this field at all wavelengths in June 2015, including its use as a phase calibrator for V404 Cyg radio observations.

2.2 Test Statistic maps and localisation

We constructed TS maps during the outburst of V404 Cyg to test whether the detection could be due to a nearby source. We show in Fig. 3 the TS map built from a 12-h integration around the date of the highest flux in the 0.1–2 GeV energy range and excluding V404 Cyg from the source model. The residual TS map shows a transient excess close to the location of V404 Cyg with a peak TS value of about 20 (∼4.5σ). The TS value drops to ∼6 if photons below 200 MeV are not considered, in agreement with the computed soft spectrum.

We used the tool `gtfindsrc` to localize the point source at the origin of the γ-ray excess emission. The best-fit location is at RA(J2000) = 305.°31, Dec. = 33.°63 with a TS of 17.6/19.5 on 6/12 h and a similar flux than reported in §2.1. The 68 and 95 per cent confidence radii are r68 = 0.°43 and r95 = 0.°69 (including corrections, 3FGL), represented as concentric circles in Fig. 3. The excess lies 0.°63 from V404 Cyg's position, 0.°84 away from the blazar B2023+336 and 1.°48 away from the next closest source, the pulsar PSR J2028+3332 (3FGL J2028.3+3332, Pletsch et al. 2012). The latter is not known to vary (variability index of 51.2, 3FGL). The position of the excess γ-ray emission thus excludes the two closest known sources. However, V404 Cyg is within the 95 per cent confidence region of the excess. The localization cannot be better constrained due to the softness of the photons, implying a larger PSF, and the short integration time, limiting the number of photons.

2.3 Hard X-ray and radio observations

In Fig. 2 we plot the V404 Cyg LCs obtained from observations with the IBIS/ISGRI imager on board the INTEGRAL satellite (data reduction similar to Rodriguez et al. 2015a). 100-s binned LCs and hardness ratios are presented in the bands 20–40 and 80–150 keV along with mean Crab levels over the year 2015 (respectively 152.9 and 33.2 ct s^{-1}).

The 15 GHz observations were obtained using the Owens Valley Radio Observatory (OVRO) 40-m telescope. Calibration is achieved using a temperature-stable diode noise source to remove receiver gain drifts and the flux density scale is derived from observations of 3C 286 (Baars et al. 1977). Details of the reduction and calibration procedure are found in Richards et al. (2011). V404 Cyg was observed with the Arcminute Microkelvin Imager (AMI-LA, 13–17 GHz), operating as part of the University of Oxford's 4 PI SKY transients programme (Fender et al., in prep.). J2025+3343 was used as phase calibrator and the absolute flux calibration was done using 3C 286 (Baars et al. 1977). The calibration and RFI excision were done using `AMI-REDUCE` (Davies et al. 2009). LCs centered at 13.9 GHz were extracted from the calibrated data via vector-averaging of the UV data.

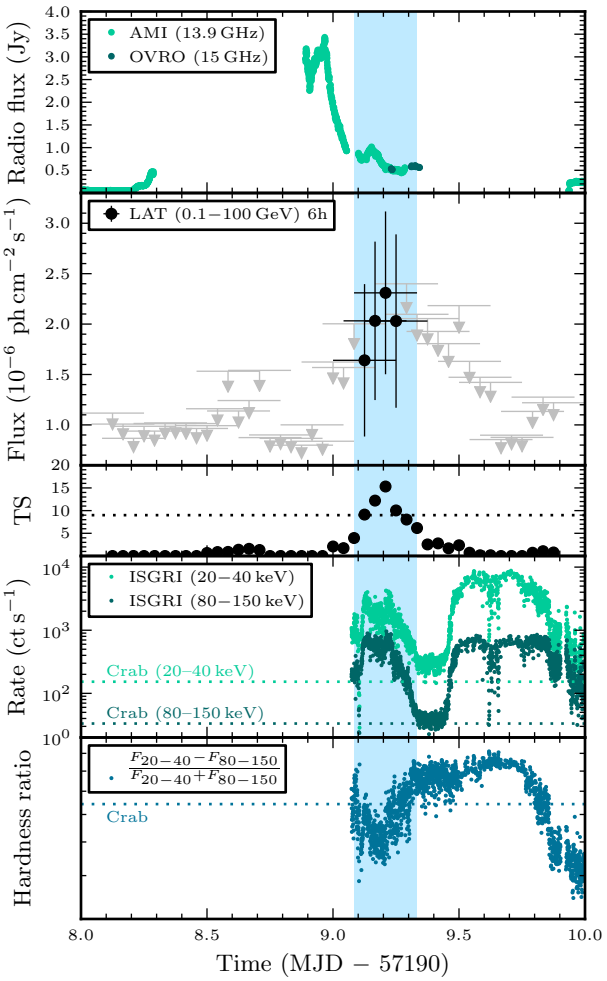

Figure 2. Multi-wavelength LC of V404 Cyg around the time of the γ-ray peak (vertical blue shaded area). From top to bottom panel: AMI and OVRO flux density evolutions; LAT flux and 95% upper limits in 6-h bins, with 1-h shifts in exposure between each measurement; corresponding TS; INTEGRAL/ISGRI (LC and hardness ratio).

3 DISCUSSION

We have found transient excess γ-ray emission at a position consistent with that of V404 Cyg, which we could not associate with a previously-known *Fermi*/LAT source. Formally, the TS of this excess is not sufficiently high to claim a detection, once the number of trials associated with constructing the LC is taken into account. The probability of measuring a TS (distributed as a χ^2_2) value $\geq$ 15.3 over the 10 days of

the outburst, given 320, 6 h-long, independent trials is ∼2%. The integrated PSF of the LAT for the soft excess seen toward V404 Cyg, in the 0.1–2 GeV band, has a 1.°5 HWHM. By comparing to 12-hour-long all-sky maps averaged before and after the time interval of the X-ray outburst, we estimate the chance probability of having a transient or fluctuation as bright as the excess at ∼2%. So, the $\sim 4 \times 10^{-4}$ probability of having a random, point-source, γ-ray excess at the time of the X-ray outburst, toward V404 Cyg supports the detection of an associated γ-ray flare. Its temporal coincidence with the brightest daily averaged *Swift*/BAT flare, associated with a marked change in the multi-wavelength properties of the source, provides a compelling reason to posit a detection of transient γ-ray emission from V404 Cyg.

3.1 Multi-wavelength behaviour

V404 Cyg showed strong flaring activity from radio to hard X-rays over a period of about 10 days following the initial detection of the outburst on MJD 57188. The brightest flares occurred at the end of this period, close in time to the detection of the γ-ray excess we report. As shown by the AMI 13.9 GHz LC (Fig. 2), a giant radio flare with a peak above 3.4 Jy occurred ∼6 h before the γ-ray flare peak. Our 15 GHz OVRO data (Fig. 2), as well as VLA and VLBA (J. Miller-Jones, priv. com.) and RATAN (Trushkin et al. 2015) observations conducted around MJD 57198 and 57200 do not indicate the presence of other major radio flares. At hard X-rays, the brightest flare reaches about 57 Crab at 20–40 keV and occurs ∼14 h after the radio flare (i.e. starting on MJD 57199.5). This is preceded by another hard X-ray flare around MJD 57199.2 that is coincident with the *Fermi*/LAT γ-ray excess. Although its 20–40 keV intensity is lower than the MJD 57199.5 flare, its 80–150 keV flux is higher (and corresponds to the maximum at ∼29 Crab over the whole outburst period, see Fig. 2). The activity on MJD 57198–57200 in radio and hard X-rays is also accompanied by the third (and last) detection of $e^- e^+$ pair annihilation (Siegert et al. 2016). The annihilation flux LC follows the 100–200 keV flux over these two days, including the dip at MJD 57199.4. The X-ray spectral fits suggest annihilation occurs in two zones with, respectively, $kT \sim 2$ keV and ∼500 keV. Siegert et al. (2016) performed a LAT study during the largest positron flare (MJD 57199.616–57200.261) and derived a 8×10^{-7} ph cm^{-2} s^{-1} upper limit that is consistent with our upper limit of 8.7×10^{-7} ph cm^{-2} s^{-1} on the same time interval, above 100 MeV. The activity and emission levels decrease markedly at all wavelengths after MJD 57200. The γ-ray excess thus appears related to the last spur of activity of the source, preceding the brightest enhancement of 511 keV emission, before it started to fade.

3.2 Gamma-ray emission from the jet?

The association of the γ-ray excess with major radio activity and marked transition to a softer X-ray state (Fig. 2) are reminiscent of Cyg X−3, where γ-ray emission is detected when the radio flux is above ∼0.2 Jy and when X-ray emission is soft – but not too much so (Corbel et al. 2012). The γ-ray luminosity from V404 Cyg is $\sim 2 \times 10^{35} (d/2.4\,\mathrm{kpc})^2$ erg s^{-1}, a factor ∼5 fainter than the typical >100 MeV luminosity from Cyg X−3. This is a minor fraction of the overall luminosity output, which reached $\sim 2 \times 10^{38}$ erg s^{-1} (Rodriguez et al. 2015a). Gamma-ray emission may thus be much fainter in V404 Cyg than in Cyg X−3, either intrinsically or because of the boosting depending on the Lorentz factor and orientation of the emission in the relativistic jet (Grenier et al. 2005). Radio VLBI imaging of the jet should be able to narrow down such a possibility. In both cases, it is likely that we have detected only the brightest flaring episode during the outburst.

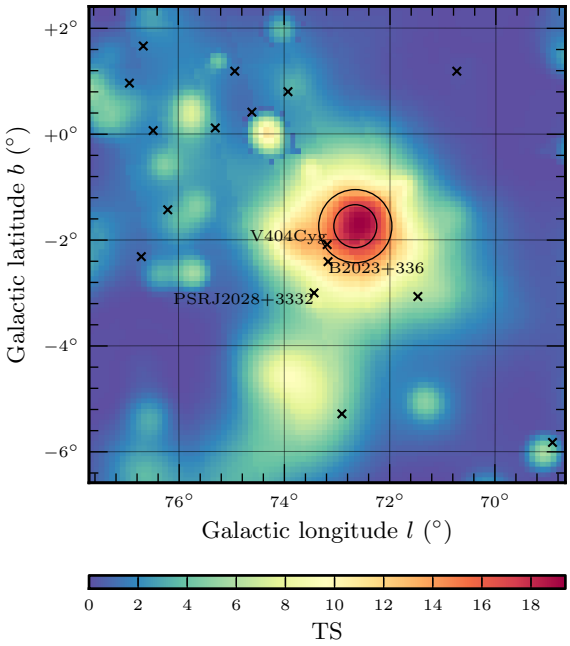

Figure 3. 12-h residual TS map on MJD 57199.25 (0.1–2 GeV, 0.°1 pixel^{-1}). 3FGL sources are marked as black crosses. 68% and 95% confidence regions on the best fit position are represented.

V404 Cyg appeared to stay in a hard or intermediate state during this outburst (Rodriguez et al. 2015a; Jenke et al. 2016; Radhika et al. 2016; Kimura et al. 2016). The tentative high-energy γ-ray detections of the microquasar Cyg X-1 are also associated with this spectral state (and/or at the transition to the soft state, Sabatini et al. 2013). Bodaghee et al. (2013) found 21 daily measurements for which TS > 9 at the position of the source, mostly when it was in a hard or intermediate state. Malyshev et al. (2013) obtained a total TS∼15 by integrating all the hard state data and no detection in the soft state. The γ-ray emission from Cyg X−1 is not a simple extrapolation of the >100 keV power-law emission detected in X-rays, associated with non-thermal emission from the corona and/or the jet (Rodriguez et al. 2015b). Models suggest that the high-energy γ-ray emission is located elsewhere, most likely associated with non-thermal emission from the jet (Malyshev et al. 2013). The association in V404 Cyg of high-energy γ-ray emission contemporaneous with annihilating $e^+ e^-$ pairs further supports this picture. Radiative models of coronal plasmas show significant 511 keV line emission when the pair energy input is primarily non-thermal and when the corona is very dense i.e. a large opacity to pair production on >100 MeV photons (e.g. Svensson 1987). The high-energy γ-ray emission must thus originate away from the corona.

An intriguing possibility is that the ejection during the radio flare is associated with the disruption of a jet extracting energy from the black hole through the Blandford-Znajek process (Blandford & Znajek 1977). Numerical simulations indicate this process to be efficient when magnetic flux dragged in by a thick accretion flow piles up to create a 'magnetically-arrested disk' (MAD) close to the black hole (Tchekhovskoy et al. 2011; McKinney et al. 2012). O' Riordan et al. (2016) show that such a configuration leads to high-energy γ-ray emission in the hard state, due to Compton upscattering of jet or disk synchrotron photons. In contrast, the γ-ray emission is very weak when the built-up magnetic flux is insufficient to suppress standard accretion. In this scenario, a transient ejection occurs when the MAD configuration is disrupted (reconnects) due to incoming magnetic flux of opposite polarity (Dexter et al. 2014). O' Riordan et al. (2016) indicate that the re-formed jet is brighter in γ-rays than prior to the major ejection. Hence, the brief γ-ray emission from V404 Cyg following a major radio flare might be associated with the temporary re-formation of a powerful Blandford-Znajek jet.

The present observations support the presence of γ-ray emission associated with ejections in microquasars, and for the first time from an accreting black hole with a low-mass donor companion. This emission is weak and variable, with a low statistical significance. Some perseverance will be required to clarify the multi-wavelength context in which it appears in this and other microquasars, thus fulfilling its potential as a diagnostic of the accretion-ejection process.

ACKNOWLEDGEMENTS

We thank J. Miller-Jones, J. Ballet and J. Perkins for useful discussions and T. Siegert for providing the annihilation LC. AL, SC and JR acknowledge funding support from the French Research National Agency: CHAOS project ANR-12-BS05-0009 and the UnivEarthS Labex program of Sorbonne Paris Cité (ANR-10-LABX-0023 and ANR-11-IDEX-0005-02). KM acknowledges funding support from the Hintze Foundation. The *Fermi*-LAT Collaboration acknowledges support for LAT development, operation and data analysis from NASA and DOE (United States), CEA/Irfu and IN2P3/CNRS (France), ASI and INFN (Italy), MEXT, KEK, and JAXA (Japan), and the K.A. Wallenberg Foundation, the Swedish Research Council and the National Space Board (Sweden). Science analysis support in the operations phase from INAF (Italy) and CNES (France) is also gratefully acknowledged. The OVRO 40-m monitoring program is supported in part by NASA grants NNX08AW31G and NNX11A043G, and NSF grants AST-0808050 and AST-1109911. We acknowledge with thanks the variable star observations from the AAVSO.

REFERENCES

Acero F., et al., 2015, ApJS, 218, 23
Ackermann M., et al., 2013, ApJ, 771, 57
Ackermann M., et al., 2015, ApJ, 810, 14
Atoyan A. M., Aharonian F. A., 1999, MNRAS, 302, 253
Atwood W. B., et al., 2009, ApJ, 697, 1071
Baars J. W. M., Genzel R., Pauliny-Toth I. I. K., Witzel A., 1977, A&A, 61, 99
Barthelmy S. D., D'Ai A., D'Avanzo P., Krimm H. A., Lien A. Y., Marshall F. E., Maselli A., Siegel M. H., 2015, GRB Coordinates Network, 17929
Beardmore A. P., Page K. L., Kuulkers E., 2015, The Astronomer's Telegram, 8455
Blandford R. D., Znajek R. L., 1977, MNRAS, 179, 433
Bodaghee A., Tomsick J. A., Pottschmidt K., Rodriguez J., Wilms J., Pooley G. G., 2013, ApJ, 775, 98
Bosch-Ramon V., Romero G. E., Paredes J. M., 2006, A&A, 447, 263
Bosch-Ramon V., Perucho M., Bordas P., 2011, A&A, 528, A89
Casares J., Charles P. A., Naylor T., 1992, Nature, 355, 614
Corbel S., Fender R. P., Tzioumis A. K., Tomsick J. A., Orosz J. A., Miller J. M., Wijnands R., Kaaret P., 2002, Science, 298, 196
Corbel S., et al., 2012, MNRAS, 421, 2947
Davies M. L., et al., 2009, MNRAS, 400, 984
Dexter J., McKinney J. C., Markoff S., Tchekhovskoy A., 2014, MNRAS, 440, 2185
Fender R., 2006, Jets from X-ray binaries. pp 381–419
Fermi LAT Collaboration et al., 2009, Science, 326, 1512
Georganopoulos M., Aharonian F. A., Kirk J. G., 2002, A&A, 388, L25
Grenier I. A., Kaufman Bernadó M. M., Romero G. E., 2005, Ap&SS, 297, 109
Helene O., 1991, Nuclear Instruments and Methods in Physics Research A, 300, 132
Jenke P. A., et al., 2016, preprint, (arXiv:1601.00911)
Kara E., et al., 2012, ApJ, 746, 159
Khargharia J., Froning C. S., Robinson E. L., 2010, ApJ, 716, 1105
Kimura M., et al., 2016, Nature, 529, 54
Krimm H. A., et al., 2013, ApJS, 209, 14
Malyshev D., Zdziarski A. A., Chernyakova M., 2013, MNRAS, 434, 2380
Mattox J. R., et al., 1996, ApJ, 461, 396
McKinney J. C., Tchekhovskoy A., Blandford R. D., 2012, MNRAS, 423, 3083
Miller-Jones J. C. A., Jonker P. G., Dhawan V., Brisken W., Rupen M. P., Nelemans G., Gallo E., 2009, ApJ, 706, L230
Mirabel I. F., Rodríguez L. F., 1999, ARA&A, 37, 409
Mooley K., Fender R., Anderson G., Staley T., Kuulkers E., Rumsey C., 2015, The Astronomer's Telegram, 7658
O' Riordan M., Pe'er A., McKinney J. C., 2016, ApJ, 819, 95
Pletsch H. J., et al., 2012, ApJ, 744, 105
Radhika D., Nandi A., Agrawal V. K., Mandal S., 2016, preprint, (arXiv:1601.03234)
Rana V., et al., 2016, ApJ, 821, 103
Richards J. L., et al., 2011, ApJS, 194, 29
Rodriguez J., et al., 2015a, A&A, 581, L9
Rodriguez J., et al., 2015b, ApJ, 807, 17
Romero G. E., Torres D. F., Kaufman Bernadó M. M., Mirabel I. F., 2003, A&A, 410, L1
Sabatini S., et al., 2013, ApJ, 766, 83
Siegert T., et al., 2016, Nature, 531, 341
Sivakoff G. R., Bahramian A., Altamirano D., Beardmore A. P., Kuulkers E., Motta S., 2015, The Astronomer's Telegram, 7959
Svensson R., 1987, MNRAS, 227, 403
Tavani M., et al., 2009, Nature, 462, 620
Tchekhovskoy A., Narayan R., McKinney J. C., 2011, MNRAS, 418, L79
Trushkin S. A., Nizhelskij N. A., Tsybulev P. G., 2015, The Astronomer's Telegram, 7716
Wagner R. M., Kreidl T. J., Howell S. B., Starrfield S. G., 1992, ApJ, 401, L97
Younes G., 2015, GRB Coordinates Network, 17932